Biofabrication Hot Paper

Deutsche Ausgabe: DOI: 10.1002/ange.201411383
Internationale Ausgabe: DOI: 10.1002/anie.201411383

# Rapid Formation of a Supramolecular Polypeptide–DNA Hydrogel for In Situ Three-Dimensional Multilayer Bioprinting**

*Chuang Li, Alan Faulkner-Jones, Alison R. Dun, Juan Jin, Ping Chen, Yongzheng Xing, Zhongqiang Yang, Zhibo Li, Wenmiao Shu,* Dongsheng Liu,* and Rory R. Duncan*

***Abstract:*** *A rapidly formed supramolecular polypeptide–DNA hydrogel was prepared and used for in situ multilayer three-dimensional bioprinting for the first time. By alternative deposition of two complementary bio-inks, designed structures can be printed. Based on their healing properties and high mechanical strengths, the printed structures are geometrically uniform without boundaries and can keep their shapes up to the millimeter scale without collapse. 3D cell printing was demonstrated to fabricate live-cell-containing structures with normal cellular functions. Together with the unique properties of biocompatibility, permeability, and biodegradability, the hydrogel becomes an ideal biomaterial for 3D bioprinting to produce designable 3D constructs for applications in tissue engineering.*

Bioprinting has attracted wide-spread attention in tissue engineering as a powerful fabrication method to design and create tissue-like structures.[1] Selecting a suitable scaffold material to be used as the bio-ink is one of the critical issues of bioprinting.[2] Hydrogels have been widely explored as scaffold materials owing to their similarities to natural extracellular matrices (ECM), thus providing a structural and physical support for cells similar to that of a natural environment.[3] To date, non-covalently cross-linked hydrogels from natural products, including alginate, chitosan, collagen, matrigel, gelatin, and agarose, have been used in vitro as scaffold materials for bioprinting;[4] however, significant limitations, including the thermal triggering of hydrogel formation, shrinking-induced shape deformations, and a lack of responsiveness and tailorability hinder their further application in 3D bioprinting with living cells. Alternatively, covalently cross-linked hydrogels from synthetic products, including poly(ethylene glycol) (PEG), polypeptides, poly(*N*-isopropylacrylamide), and pluronics, have emerged as appealing candidates because of their clear molecular structures with possibilities to fine-tune their responsive properties.[5] However, several drawbacks, such as harsh reaction conditions, a lack of specific biodegradability and biocompatibility, and the inability of self-healing between layers, have limited their applications in in situ multilayer 3D bioprinting with living cells. Therefore, the development of novel bioprintable scaffold materials that overcome the above-mentioned limitations is urgently needed, but remains challenging. DNA is an excellent building scaffold to construct versatile devices and materials,[6] especially DNA hydrogels, which possess several advantages, such as designable responsiveness (e.g., to the pH value, temperature, the presence of enzymes and aptamers, or light),[7] non-swelling/non-shrinking properties, biodegradability, and the permeability of nutrients.[7f] Previously reported applications, such as cell-free protein production,[8] covers for single-cell capture and release,[7f] and ion detection,[7d,9] were only based on some of these properties. However, applications that combine all of these unique properties and fulfill the requirements for 3D bioprinting have not been explored to date.

Herein, we report the first method for rapid in situ multilayer 3D bioprinting with DNA-based hydrogels as bio-inks. As shown in Scheme 1, the DNA hydrogel contains two components: A polypeptide–DNA conjugate (bio-ink **A**) and a complementary DNA linker (bio-ink **B**). The mixing of bio-ink **A** and bio-ink **B** in a desired molar ratio leads to rapid in situ hydrogel formation (within seconds) owing to DNA hybridization. By alternative deposition of bio-ink **A** and bio-ink **B** in the programmed position, designed 3D structures containing viable and functional living cells could be constructed. The resultant hydrogel combines favorable properties of both the polypeptide and DNA components, that is, it is responsive to proteases and nucleases, leading to full biodegradability and programmability of the hydrogel networks under physiological conditions.

[*] C. Li, Dr. J. Jin, Dr. Y. Xing, Prof. Z. Yang, Prof. D. Liu
Key Laboratory of Organic Optoelectronics & Molecular Engineering of the Ministry of Education
Department of Chemistry
Tsinghua University, Beijing 100084 (China)
E-mail: liudongsheng@tsinghua.edu.cn

A. Faulkner-Jones, Dr. A. R. Dun, Dr. W. Shu, Prof. R. R. Duncan
Institute of Biological Chemistry, Biophysics and Bioengineering
Heriot-Watt University, Edinburgh EH14 4AS (UK)
E-mail: w.shu@hw.ac.uk

Dr. P. Chen, Prof. Z. Li
Beijing National Laboratory for Molecular Sciences (BNLMS)
Institute of Chemistry, Chinese Academy of Sciences
Beijing 100190 (China)

[**] We thank the National Basic Research Program of China (973 program, 2013CB932803), the National Natural Science Foundation of China (91427302, 21421064), the NSFC–DFG joint project TRR61, and the Beijing Municipal Science & Technology Commission for financial support. This project was also partly supported by the Sino–UK Higher Education Research Partnership for PhD Studies Scheme funded by the British Council and the Ministry of Education in China and EPSRC (EP/M506837/1) and MRC awards to R.R.D. (MRC_G0901607) and by the Wellcome Trust (WT074146). The MRC (MRC_MR/K01563X/1) Edinburgh Super-Resolution Imaging Consortium (ESRIC) provided the microscope platforms, technical assistance, tissue culturing facilities, and analysis packages required for the acquisition and analysis of fluorescence imaging data summarized in this article.

Supporting information for this article is available on the WWW under http://dx.doi.org/10.1002/anie.201411383.

  

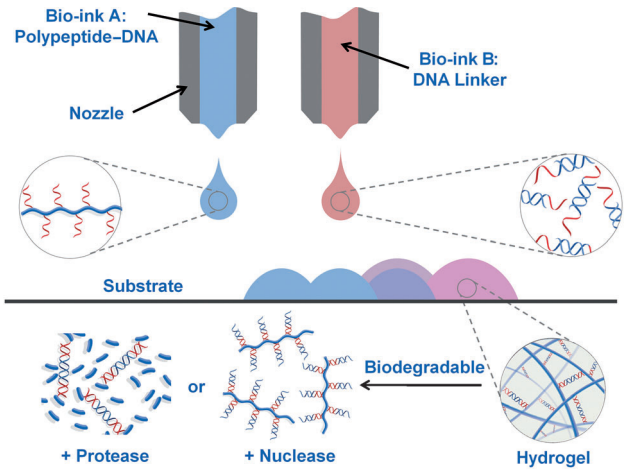


***Scheme 1.*** 3D bioprinting of the polypeptide–DNA hydrogel to fabricate arbitrarily designed 3D structures. Bio-ink **A** (blue): polypeptide–DNA, bio-ink **B** (red): DNA linker. The DNA sequences of bio-ink **A** and bio-ink **B** are complementary, and hybridization will cause crosslinking, leading to hydrogel formation (pink). The formed hydrogels are responsive to both proteases and nucleases, resulting in the full on-demand degradation of the hydrogel networks after printing.

As illustrated in Figure 1 a, the hydrogel can be fabricated by a two-component mixing strategy: Bio-ink **A** is a polypeptide–DNA conjugate, which was synthesized by grafting multiple single-stranded DNAs (ssDNAs) onto a polypeptide backbone by a copper(I)-catalyzed click reaction between azide–DNA and poly(L-glutamic acid$_{240}$-*co*-γ-propargyl-L-glutamate$_{20}$) (p(LGA$_{240}$-*co*-PLG$_{20}$), $M_w = 34060$, PDI 1.4) following an established method (see the Supporting Information, Scheme S1).[7i] On average, five to six ssDNA motifs were conjugated to each polypeptide backbone (Figure S1), resulting in a sufficient number of crosslinking points. In contrast, bio-ink **B** is a double-stranded DNA (dsDNA) containing two "sticky ends" with exactly the same sequences (Figure S2), which are complementary to those of the ssDNA motifs grafted onto the polypeptides in bio-ink **A** (for the exact sequences, see Table S1). It was found that a mixture (5 wt%) of the two bio-inks with a 1:1 molar ratio of sticky ends in 1× TBE buffer (pH 8.3, NaCl concentration: 200 mM; TBE = Tris-borate-EDTA) rapidly changed from a fluidic solution into an optically transparent supramolecularly cross-linked network within seconds, namely a polypeptide–DNA hydrogel (Figure 1 a). Notably, the hydrogel could be formed under physiological conditions (e.g., [NaCl] = 150 mM, PBS buffer, pH 7.4, 37 °C; see Figure S3), which is desirable for applications where the hydrogels have to be formed in situ with living cells. The hydrogel formation was further characterized using a shear rheometer, and $G'$ was found to be significantly higher than $G''$ over the entire frequency range (Figure 1 b), indicating that the hydrogel had indeed been formed as designed. The $G'$ value was determined to be very high (ca. 5000 Pa), resulting in a self-supported and free-standing hydrogel up to the millimeter scale (Figure 1 a).

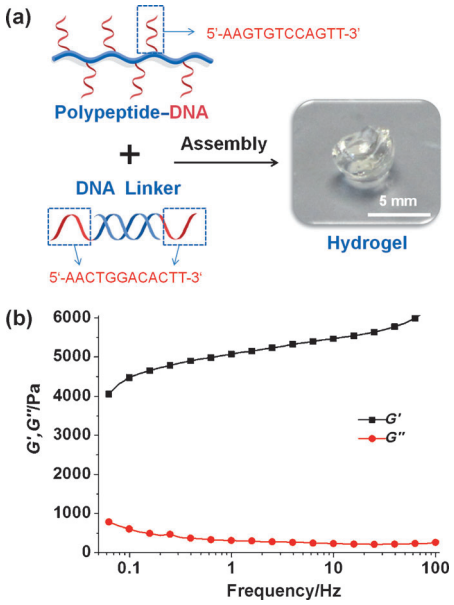


***Figure 1.*** a) Preparation of the polypeptide–DNA hydrogel by the two-component mixing of bio-inks **A** and **B**. b) Rheological characterization of a hydrogel (5 wt%). The frequency sweep was carried out between 0.05 and 100 Hz at a fixed strain of 1% at 25 °C.

The unique two-component mixing strategy and the rapid hydrogel formation can fulfil the requirements for 3D bioprinting, which is a promising free-form fabrication method to produce tissue-like structures.[4e] Therefore, equal amounts of bio-ink **A** (polypeptide–DNA, 6 wt%, 100 μL) and bio-ink **B** (DNA linker, 2 mM, 100 μL) were loaded into two separate printing cartridges of a microvalve-based 3D bioprinter, which was able to print in 3D human pluripotent stem cells whilst maintaining cell viability and function.[10] By alternatively printing microdroplets of bio-ink **A** and bio-ink **B** on the same spot, immediate contact and mixing of the printed nanoliter droplets led to rapid in situ hydrogel formation by DNA hybridization. Different 3D tissue-like patterns and structures with desired scales and dimensions could be constructed with the bioprinter based on this bottom-up assembly strategy. Figure 2 a shows a printed array of hydrogel droplets with an increasing gradient of sizes with blue dye added for visualization. The smallest printed hydrogel droplet was estimated to have a diameter of approximately 500 μm, a thickness of 80 μm, and a volume of 60 nL. The formation of the 3D printed hydrogel was very rapid (completed within 1 s), which is significantly faster than hydrogel formation after manual mixing (e.g., within several seconds). This is probably facilitated by the small volume of the printed droplets and hence smaller diffusion distances. Interestingly, the volume and scale of one hydrogel droplet can be precisely controlled, and the locations of and distances between different hydrogel droplets can be geometrically tuned by designing the required programs. Owing to cross-linking by the rigid DNA duplex, the printed hydrogel droplets show no obvious shrinking or swelling phenomena, avoiding the possibility of shape deformation after printing. Furthermore, hydrogel droplets with 20 layers of printed inks were found to be mechanically strong enough to be manipulated physically (Figure 2 a, inset). Apart from the droplet

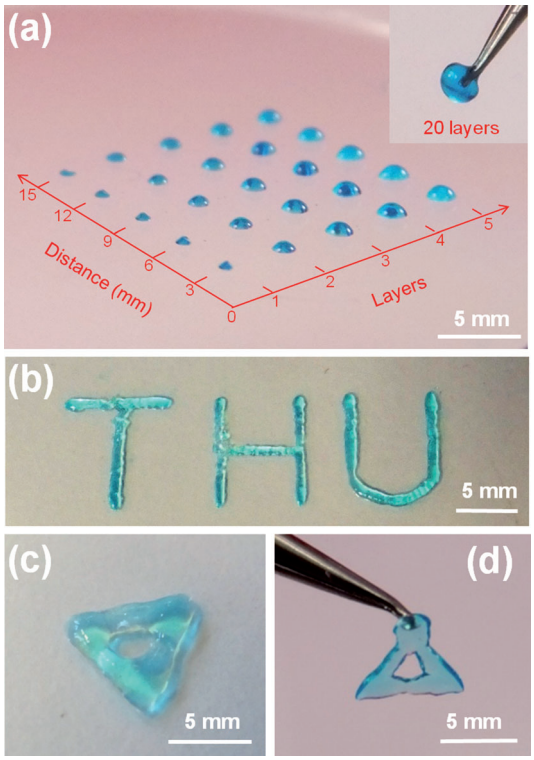


***Figure 2.*** 3D printing of polypeptide–DNA hydrogels into 3D structures with a blue dye added for visualization. a) An array of printed droplets with an increasing number of layers (up to 5 layers). Inset: Hydrogel structure with 20 layers. b) The letters "THU" printed with five layers. c, d) A triangle with ten layers, which was printed in five minutes. d) Rhe printed hydrogel structure is strong enough to be picked up with tweezers.

arrays, designable hydrogel structures, such as the letters "THU" with five layers (Figure 2b) and a simple triangle with ten layers (Figure 2c) were 3D printed, demonstrating the ability of our system to print arbitrary 3D structures. One layer of the triangle could be prepared in 30 s, indicating that our printing strategy is a rapid fabrication method for millimeter-sized objects. The triangular hydrogel structure (Figure 2d) could be manipulated without collapse, indicating that the mechanical strength of the 3D printed hydrogel is strong enough to support its printed shapes. Furthermore, the printed structures are optically transparent and geometrically uniform without obvious boundaries between the printed layers. This is due to the fact that the contacting layers of the hydrogel can further merge and heal together based on the supramolecular dynamic cross-linking of DNA hybridization. All of these unique properties make our hydrogel a promising printing material for the fabrication of complex 3D constructs with precise inner structures.

Furthermore, we used the hydrogels in cell printing, which offers the possibility to build 3D structures of cells (Figure 3a).[1a] AtT-20 cells (an anterior pituitary cell line) were chosen as the model cell line.[11] On addition of the AtT-20 cells, the bio-inks maintained them in a stable and homogenous cell suspension, preventing the cell settlement and aggregation that commonly impede cell printing. This may be an unexpected advantage of the specific viscosity and surface tension of the bio-inks, which not only help maintain the cells in a suspension, but also meet the stringent requirements in terms of fluid properties needed for bioprinting with a nozzle-based technique. We performed a thorough characterization of the viability and function of the AtT-20 cells after printing within the 3D hydrogel. Figure 3b shows a 3D stack of printed AtT-20 cells in a hydrogel stained with fluorescein diacetate (FDA); a live/dead assay gave a viability of $98.8 \pm 1.4\,\%$ (mean $\pm$ SD), indicating that the printing process apparently caused negligible damage to the cells. To test the biological functions of the printed cells, we also monitored single cells in the hydrogel stained with Lysotracker Red at a high resolution over time, revealing intracellular acidic compartments (in red; Figure 3c). These intracellular acidic compartments (including lysosomes and large dense-cored vesicles) were visualized within the cytosol of a printed AtT20 cell using an inverted wide-field microscope (Figure 3d) and were tracked over time (Figure 3e). The organelle dynamics indicated that the printed AtT-20 cells were viable, had a normal 3D morphology, and exhibited various cellular functions, including proton pump activity, metabolic turnover, and membrane

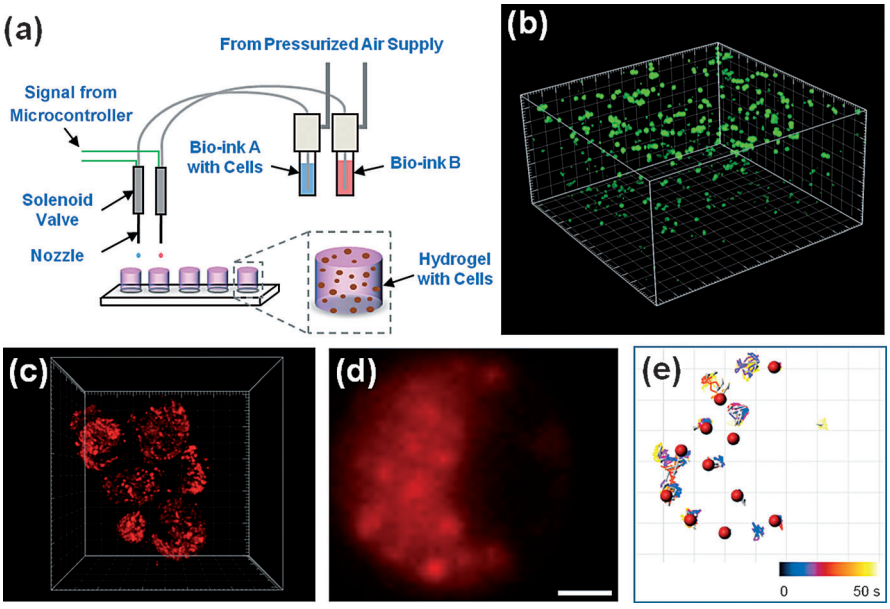


***Figure 3.*** 3D bioprinting of polypeptide–DNA hydrogels with AtT-20 cells. a) Cell-printing process based on ink-jet techniques. b, c) 3D stacks of AtT-20 cells printed in a hydrogel with FDA staining in green (gridlines: 50 µm; b) or Lysotracker Red staining in red (gridlines: 5 µm; c). d) A single cell was imaged using wide-field microscopy, a cross section of the cells shows acidic compartments. Scale bar: 1 µm. e) Dynamic organelles were tracked and trajectories from inside the cell in (d) are shown. The tracked organelles are shown as red spheres and tracks as colored lines with displacements indicated by gray arrows. The color bar and the colors of the tracks represent the time (0–50 s). Gridlines: 1 µm.

trafficking.[12] Next, cell cultures of two types of cells (AtT-20 and HEK-293 cells) were monitored for a prolonged period of time, which showed that the cells maintained their high viability (Figure S5), demonstrating that the hydrogel is mechanically strong enough to provide physical support for the encapsulated cells, non-toxic to cells, and permeable for nutrients, which are desirable properties for the long-term use of cell cultures.

We then studied the biodegradability of our hydrogel, which is a crucial and desirable property for bioprinting. It was found that protease (endoproteinase Glu-C, 30 U) can degrade the polypeptide backbone, which leads to the collapse of the hydrogel (5 wt%; Figure 4, tube 2) after

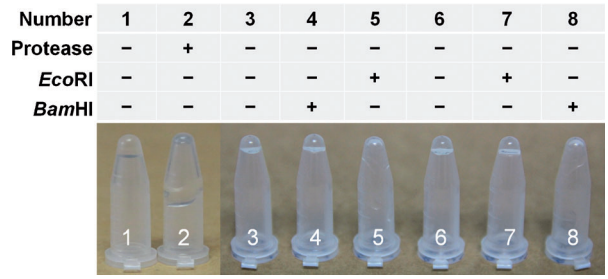


***Figure 4.*** Enzymatic degradation of the polypeptide–DNA hydrogels. Tubes 1 and 2: Protease responsiveness. The hydrogel (5 wt%, 10 μL) was incubated in phosphate buffer (pH 7.8, 10 μL) without protease (1) or with 30 U endoproteinase Glu-C (2) at room temperature for 12 hours. Tubes 3–8: Nuclease responsiveness. Hydrogel "R" (3–5) and hydrogel "H" (6–8) contain the restriction sequences of *Eco*RI and *Bam*HI on their linkers, respectively. In the tubes, the hydrogel (5 wt%, 10 μL) was incubated in a buffer solution (10 μL) without enzymes (tubes 3 and 6), with 30 U of *Bam*HI (tubes 4 and 8), or with 30 U of *Eco*RI (tubes 5 and 7) at room temperature for 24 hours.

incubation for twelve hours. Alternatively, a nuclease can cleave the DNA linkers and specifically digest the hydrogel network. For example, after incubation for 24 hours, hydrogels containing *Eco*RI (or *Bam*HI) restriction sites remained in the gel state in the absence of *Eco*RI (tubes 3 and 4; or in the absence of *Bam*HI, tubes 6 and 7), but turned into a solution when digested by *Eco*RI (in tube 5; or by *Bam*HI, tube 8). These results indicate that the hydrogels possess specific dual-enzymatic responsiveness to both proteases and nucleases, which cannot only fully biodegrade both the hydrogel backbone and the cross-linker, but also offer the possibility of selectively removing parts of the hydrogel in the presence of cells to obtain specific 3D and heterogeneous tissue structures.[13]

In summary, we have reported the rapid formation of a supramolecular polypeptide–DNA hydrogel, which was subsequently used for in situ multilayer 3D bioprinting for the first time. Because of dynamic cross-linking by DNA hybridization, the printed hydrogels possess excellent healing properties, resulting in geometrically uniform constructs without boundaries. Furthermore, the printed structures can keep their shapes up to the millimeter scale without collapse benefiting from the high mechanical strength and the non-swelling/shrinking properties of the hydrogel. Cell printing was demonstrated to produce structures containing viable cells with normal cellular functions. As the hydrogel is also biocompatible with cells, permeable to nutrients, and biodegradable, it is a new promising printable biomaterial for the fabrication of complex three-dimensional tissue-like constructs in tissue engineering.

**Keywords:** biodegradability · DNA structures · hydrogels · polypeptides · supramolecular chemistry

**Zitierweise:** *Angew. Chem. Int. Ed.* **2015**, *54*, 3957–3961
*Angew. Chem.* **2015**, *127*, 4029–4033

[1] a) P. Calvert, *Science* **2007**, *318*, 208–209; b) S. V. Murphy, A. Atala, *Nat. Biotechnol.* **2014**, *32*, 773–785; c) M. D. Symes, P. J. Kitson, J. Yan, C. J. Richmond, G. J. T. Cooper, R. W. Bowman, T. Vilbrandt, L. Cronin, *Nat. Chem.* **2012**, *4*, 349–354; d) N. G. Durmus, S. Tasoglu, U. Demirci, *Nat. Mater.* **2013**, *12*, 478–479; e) X. Tao, W. B. Kyle, Z. A. Mohammad, D. Dennis, Z. Weixin, J. Y. James, A. Anthony, *Biofabrication* **2013**, *5*, 015001.

[2] a) S. V. Murphy, A. Skardal, A. Atala, *J. Biomed. Mater. Res. A.* **2013**, *101A*, 272–284; b) M. Nakamura, S. Iwanaga, C. Henmi, K. Arai, Y. Nishiyama, *BioFactors* **2010**, *2*, 014110; c) F. Pati, J. Jang, D.-H. Ha, S. Won Kim, J.-W. Rhie, J.-H. Shim, D.-H. Kim, D.-W. Cho, *Nat. Commun.* **2014**, *5*, 3935; d) L. Riccardo, V. Jetze, A. P. Josep, E. Elisabeth, M. Jos, A. M.-T. Miguel, *Biofabrication* **2014**, *6*, 035020.

[3] a) D. Seliktar, *Science* **2012**, *336*, 1124–1128; b) M. P. Lutolf, P. M. Gilbert, H. M. Blau, *Nature* **2009**, *462*, 433–441; c) J. L. Drury, D. J. Mooney, *Biomaterials* **2003**, *24*, 4337–4351; d) B. V. Slaughter, S. S. Khurshid, O. Z. Fisher, A. Khademhosseini, N. A. Peppas, *Adv. Mater.* **2009**, *21*, 3307–3329; e) E. A. Appel, J. del Barrio, X. J. Loh, O. A. Scherman, *Chem. Soc. Rev.* **2012**, *41*, 6195–6214; f) G. A. Silva, C. Czeisler, K. L. Niece, E. Beniash, D. A. Harrington, J. A. Kessler, S. I. Stupp, *Science* **2004**, *303*, 1352–1355; g) Y. Zhang, L. Tao, S. Li, Y. Wei, *Biomacromolecules* **2011**, *12*, 2894–2901.

[4] a) G. Hemanth, Y. Jingyuan, H. Yong, B. C. Douglas, *Biofabrication* **2014**, *6*, 035022; b) S. Khalil, W. Sun, *J. Biomech. Eng.* **2009**, *131*, 111002; c) J. C. Reichert, A. Heymer, A. Berner, J. Eulert, U. Nöth, *Biomed. Mater.* **2009**, *4*, 065001; d) K. Pataky, T. Braschler, A. Negro, P. Renaud, M. P. Lutolf, J. Brugger, *Adv. Mater.* **2012**, *24*, 391–396; e) T. Xu, J. Jin, C. Gregory, J. J. Hickman, T. Boland, *Biomaterials* **2005**, *26*, 93–99; f) K. Haruka, S. Takao, F. Tsuyohiko, N. Naotoshi, N. Kohji, *Biofabrication* **2013**, *5*, 015010.

[5] a) R. Censi, W. Schuurman, J. Malda, G. di Dato, P. E. Burgisser, W. J. A. Dhert, C. F. van Nostrum, P. di Martino, T. Vermonden, W. E. Hennink, *Adv. Funct. Mater.* **2011**, *21*, 1833–1842; b) K. Nagahama, T. Ouchi, Y. Ohya, *Adv. Funct. Mater.* **2008**, *18*, 1220–1231; c) M. Chaouat, C. Le Visage, W. E. Baille, B. Escoubet, F. Chaubet, M. A. Mateescu, D. Letourneur, *Adv. Funct. Mater.* **2008**, *18*, 2855–2861; d) J. Malda, J. Visser, F. P. Melchels, T. Jüngst, W. E. Hennink, W. J. A. Dhert, J. Groll, D. W. Hutmacher, *Adv. Mater.* **2013**, *25*, 5011–5028.

[6] a) N. C. Seeman, *Nature* **2003**, *421*, 427–431; b) S. Peng, T. L. Derrien, J. Cui, C. Xu, D. Luo, *Mater. Today* **2012**, *15*, 190–194; c) D. Liu, E. Cheng, Z. Yang, *NPG Asia Mater.* **2011**, *3*, 109–114; d) Y. Dong, Z. Yang, D. Liu, *Acc. Chem. Res.* **2014**, *47*, 1853–1860; e) S. Modi, M. G. Swetha, D. Goswami, G. D. Gupta, S. Mayor, Y. Krishnan, *Nat. Nanotechnol.* **2009**, *4*, 325–330; f) A. V. Pinheiro, D. Han, W. M. Shih, H. Yan, *Nat. Nanotechnol.* **2011**, *6*, 763–772; g) J. Bath, A. J. Turberfield, *Nat. Nanotechnol.* **2007**, *2*, 275–284; h) Y. Ke, L. L. Ong, W. M. Shih, P. Yin, *Science* **2012**, *338*, 1177–1183; i) N. Chen, J. Li, H. Song, J. Chao, Q. Huang, C. Fan, *Acc. Chem. Res.* **2014**, *47*, 1720–1730.

  

[7] a) S. H. Um, J. B. Lee, N. Park, S. Y. Kwon, C. C. Umbach, D. Luo, *Nat. Mater.* **2006**, *5*, 797 – 801; b) B. Wei, I. Cheng, K. Q. Luo, Y. Mi, *Angew. Chem. Int. Ed.* **2008**, *47*, 331 – 333; *Angew. Chem.* **2008**, *120*, 337 – 339; c) E. Cheng, Y. Xing, P. Chen, Y. Yang, Y. Sun, D. Zhou, L. Xu, Q. Fan, D. Liu, *Angew. Chem. Int. Ed.* **2009**, *48*, 7660 – 7663; *Angew. Chem.* **2009**, *121*, 7796 – 7799; d) Z. Zhu, C. Wu, H. Liu, Y. Zou, X. Zhang, H. Kang, C. J. Yang, W. Tan, *Angew. Chem. Int. Ed.* **2010**, *49*, 1052 – 1056; *Angew. Chem.* **2010**, *122*, 1070 – 1074; e) Y. Xing, E. Cheng, Y. Yang, P. Chen, T. Zhang, Y. Sun, Z. Yang, D. Liu, *Adv. Mater.* **2011**, *23*, 1117 – 1121; f) J. Jin, Y. Xing, Y. Xi, X. Liu, T. Zhou, X. Ma, Z. Yang, S. Wang, D. Liu, *Adv. Mater.* **2013**, *25*, 4714 – 4717; g) P. Chen, C. Li, D. Liu, Z. Li, *Macromolecules* **2012**, *45*, 9579 – 9584; h) H. Qi, M. Ghodousi, Y. Du, C. Grun, H. Bae, P. Yin, A. Khademhosseini, *Nat. Commun.* **2013**, *4*, 2275; i) C. Li, P. Chen, Y. Shao, X. Zhou, Y. Wu, Z. Yang, Z. Li, T. Weil, D. Liu, *Small* **2015**, DOI: 10.1002/smll.201401906; j) J. Liu, *Soft Matter* **2011**, *7*, 6757 – 6767; k) Y. Wu, C. Li, F. Boldt, Y. Wang, S. L. Kuan, T. T. Tran, V. Mikhalevich, C. Fortsch, H. Barth, Z. Yang, D. Liu, T. Weil, *Chem. Commun.* **2014**, *50*, 14620 – 14622; l) E. Cheng, Y. Li, Z. Yang, Z. Deng, D. Liu, *Chem. Commun.* **2011**, *47*, 5545 – 5547.

[8] N. Park, S. H. Um, H. Funabashi, J. Xu, D. Luo, *Nat. Mater.* **2009**, *8*, 432 – 437.

[9] N. Dave, M. Y. Chan, P.-J. J. Huang, B. D. Smith, J. Liu, *J. Am. Chem. Soc.* **2010**, *132*, 12668 – 12673.

[10] A. Faulkner-Jones, S. Greenhough, J. A. King, J. Gardner, A. Courtney, W. Shu, *Biofabrication* **2013**, *5*, 015013.

[11] M. J. Shipston, R. R. Duncan, A. G. Clark, F. A. Antoni, L. Tian, *Mol. Endocrinol.* **1999**, *13*, 1728 – 1737.

[12] L. Yang, A. R. Dun, K. J. Martin, Z. Qiu, A. Dunn, G. J. Lord, W. Lu, R. R. Duncan, C. Rickman, *PLoS One* **2012**, *7*, e49514.

[13] a) Y.-C. Chiu, J. C. Larson, V. H. Perez-Luna, E. M. Brey, *Chem. Mater.* **2009**, *21*, 1677 – 1682; b) L. A. Hockaday, K. H. Kang, N. W. Colangelo, P. Y. C. Cheung, B. Duan, E. Malone, J. Wu, L. N. Girardi, L. J. Bonassar, H. Lipson, C. C. Chu, J. T. Butcher, *Biofabrication* **2012**, *4*, 035005.

Received: November 24, 2014
Revised: December 26, 2014
Published online: February 5, 2015

  